

# Chemical and Microstructural Effects in Electrode Polarization

Anil V. Virkar

University of Utah and Materials and  
Systems Research, Inc. (MSRI)

List of Contributors: Tad Armstrong, Rajesh Radhakrishnan,  
G. Ramanan and Feng Zhao - UofU and MSRI  
Subhash Singhal - PNNL

Presented at SECA Core Technology Workshop  
January 27 & 28, 2005  
Tampa, Florida

Supported in part by the U. S. Department of Energy  
Under Contract No. DE-FC26-02NT41602

Part of the work done using EMSL Facilities at PNNL

# Outline

- A relative comparison of contributions of the various polarizations in anode-supported cells. Comparison of experimental results with a model.
- Concentration polarization in Anode-Supported Cells: Electrode thickness and microstructure effects.
- Effect of Morphology on Ion Transport through Porous Bodies and Activation Polarization.
- Cathode Activation Polarization: Charge Transfer Studies using Patterned Electrodes: LSM/YSZ and Pt/YSZ. Effect of oxygen partial pressure and temperature.
- Patterned Electrodes for the Study of Cathode Poisoning by chromium.
- Surface exchange coefficient measurements on porous MIEC samples.
- Summary.

# Chemical and Microstructural Effects

- Chemical

- a) Material Composition
- b) Defect Chemistry
- c) Gas/Solid Interactions
- d) Charge Transfer
- e) Transport

- Microstructural

- a) Porosity
- b) Pore Size
- c) Tortuosity
- d) Thickness
- e) Three-Phase Boundary
- f) Specific Surface Area
- g) Particle Size
- h) Inter-Particle Neck Size

# Approximate Values of the Various Polarizations $\eta$ in Anode-Supported Cells

Various contributions at 800°C, at 1 A/cm<sup>2</sup>, low fuel utilization  
For a standard, medium performance anode-supported cell

$$\eta_{ohmic} \sim 150 \text{ mV}$$

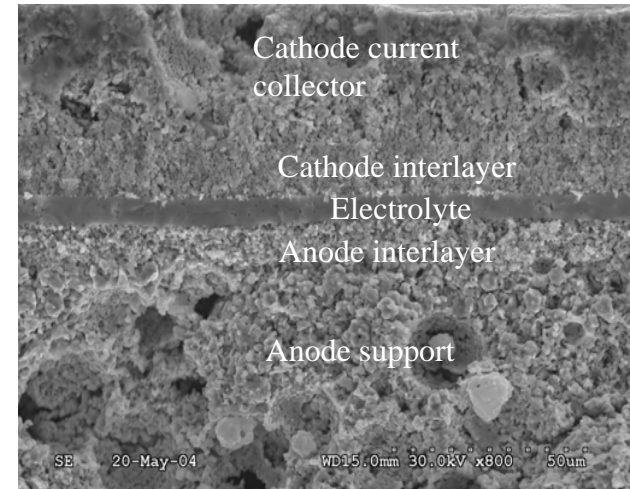
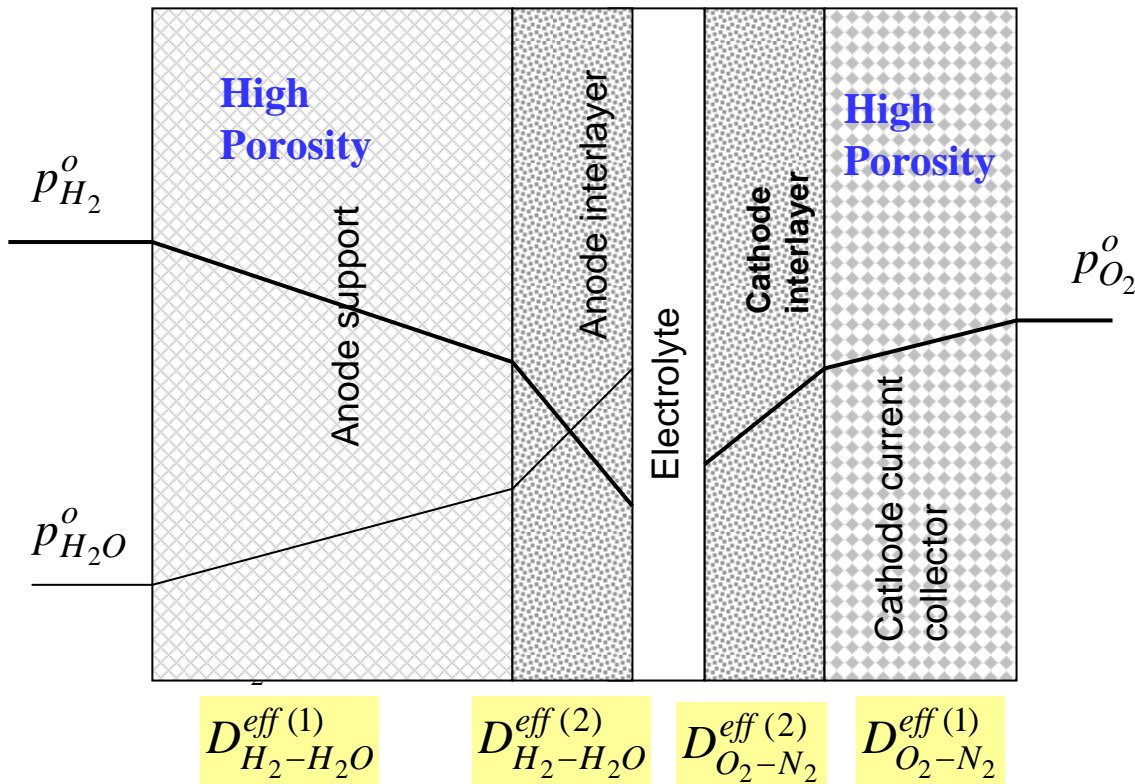
$$\eta_{anode-concentration} \sim 125 \text{ mV}$$

$$\eta_{cathode-concentration} \sim 10 \text{ mV}$$

$$\eta_{activation} \sim 100 \text{ mV}$$

The corresponding cell performance at ~0.7 V is ~0.7 W/cm<sup>2</sup>

# A Five Layer Anode-Supported Cell



**Cell performance  
almost identical in  $H_2$   
and  $H_2 + CO$  mixtures  
if  $p_{CO} < p_{H_2}$**

## Parameters which dictate Concentration Polarization (typical values)

- 1) Electrode porosity (25 to 60%)
- 2) Electrode pore size (a few microns)
- 3) Electrode tortuosity (3 to 15 – high values include Knudsen diffusion)
- 4) Gas phase diffusivities (1 to 5  $cm^2/s$ )
- 5) Electrode thickness (50 microns to 2 mm)

# A Simple, Phenomenological Polarization Equation in Terms of Experimentally Measurable Parameters

$$V(i) = E_0 - iR_i - a - b \ln i + \frac{RT}{2F} \ln \left( \frac{p'_{H_2(i)}(i) p^o_{H_2O}}{p^o_{H_2} p'_{H_2O(i)}(i)} \right) + \frac{RT}{4F} \ln \left( \frac{p'_{O_2(i)}(i)}{p^o_{O_2}} \right)$$

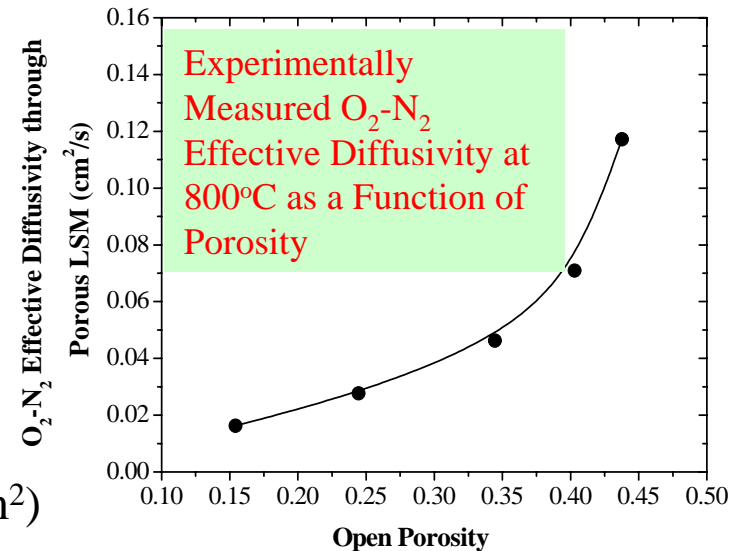
$E_0$  = Nernst Voltage

$R_i$  = Ohmic Area Specific Resistance ( $\Omega\text{cm}^2$ )

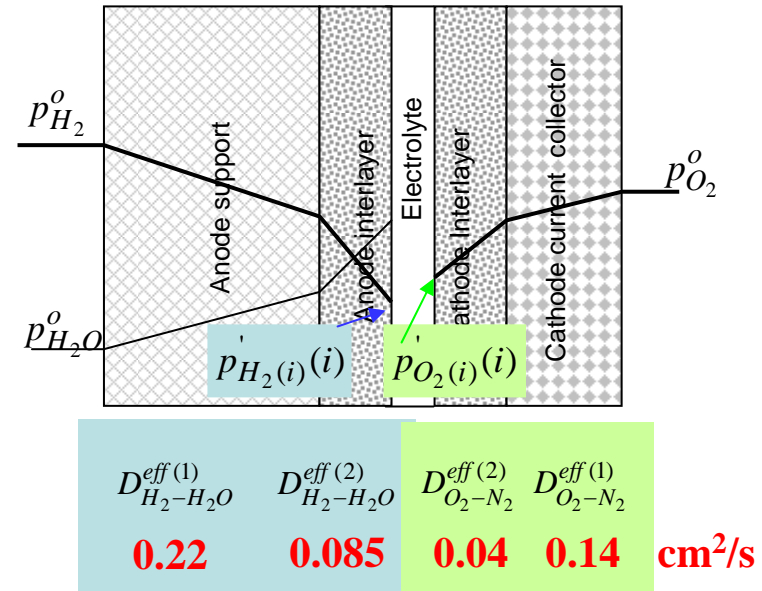
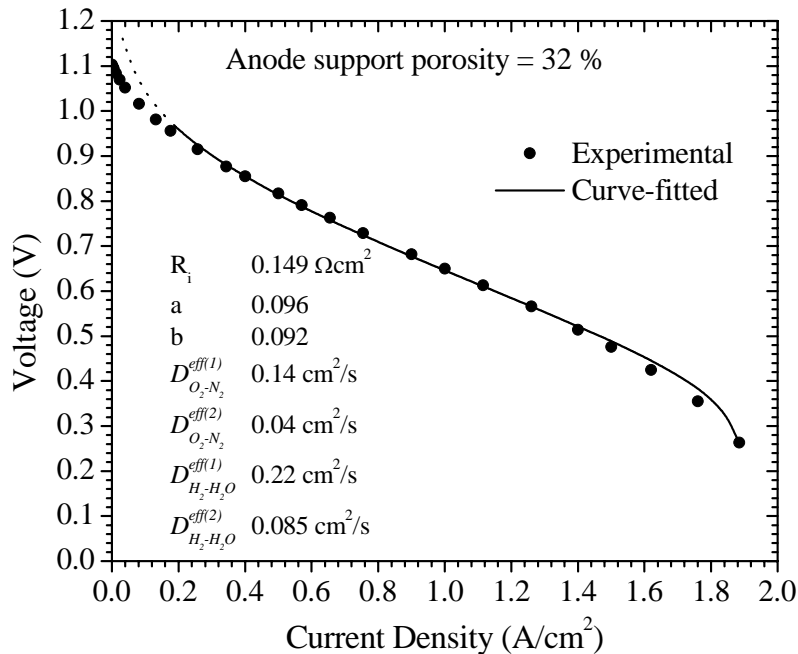
$a, b$  = Tafel Coefficients

$p'_{H_2(i)}(i)$  = Partial pressure of hydrogen at anode/electrolyte interface. Depends on Measurable Effective Diffusivity through porous anode

$p'_{O_2(i)}(i)$  = Partial pressure of oxygen at cathode/electrolyte interface. Depends on Measurable Effective Diffusivity through porous cathode



# Fitting the Model to Experimental Results



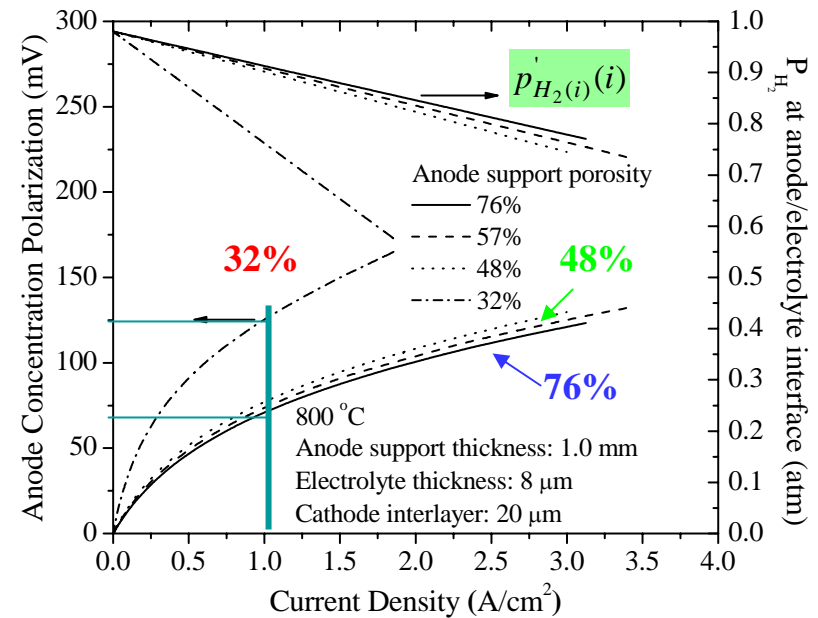
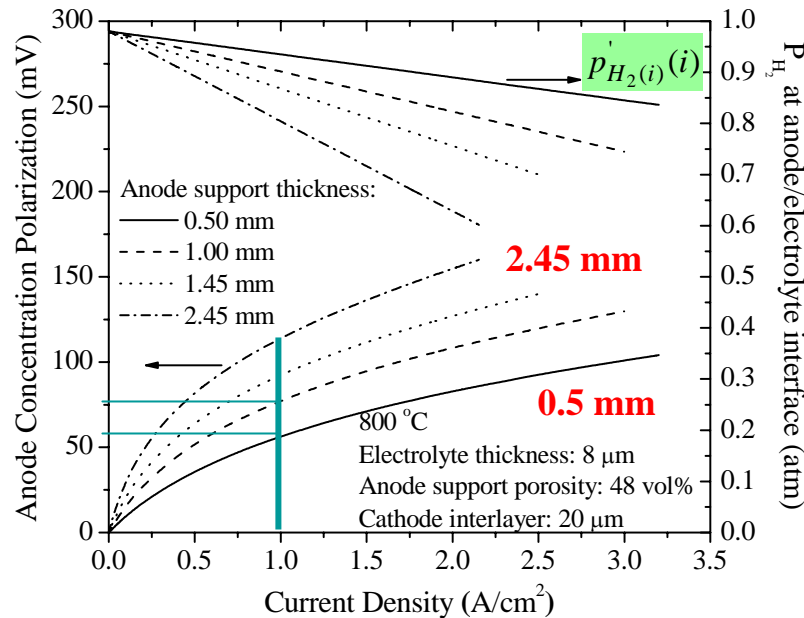
$$V(i) = E_0 - \underbrace{iR_i}_{\text{ohmic}} - \underbrace{a - b \ln i}_{\text{activation}} + \frac{RT}{2F} \ln \left( \frac{p'_{H_2(i)}(i) p_{H_2O}^o}{p_{H_2}^o p_{H_2O(i)}(i)} \right) + \frac{RT}{4F} \ln \left( \frac{p_{O_2(i)}(i)}{p_{O_2}^o} \right)$$

← anode concentration →
← cathode concentration →

$p'_{H_2(i)}(i)$  and  $p_{H_2O(i)}(i)$  depend on  $D_{H_2-H_2O}^{eff(1)}$  and  $D_{H_2-H_2O}^{eff(2)}$  and thicknesses

$p_{O_2(i)}(i)$  depends on  $D_{O_2-N_2}^{eff(1)}$  and  $D_{O_2-N_2}^{eff(2)}$  and thicknesses

# Anode Concentration Polarization: Effect of Porosity and Thickness



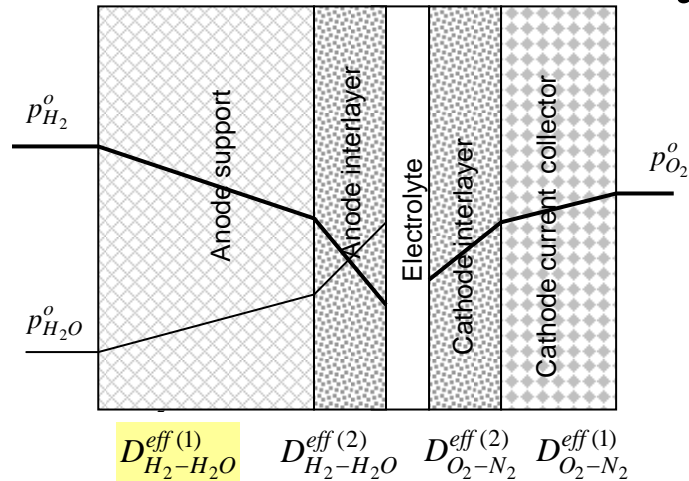
Anode Porosity <b>48%</b> Thickness Varied	Anode (0% Fuel Util.) Concentration Polarization at 1 $\text{A}/\text{cm}^2$
0.5 mm	55 mV
1.0 mm	75 mV
1.45 mm	90 mV
2.45 mm	115 mV

Anode Thickness <b>1 mm</b> Porosity Varied	Anode (0% Fuel Util.) Concentration Polarization at 1 $\text{A}/\text{cm}^2$
32%	125 mV
48%	75 mV
57%	72 mV
76%	70 mV

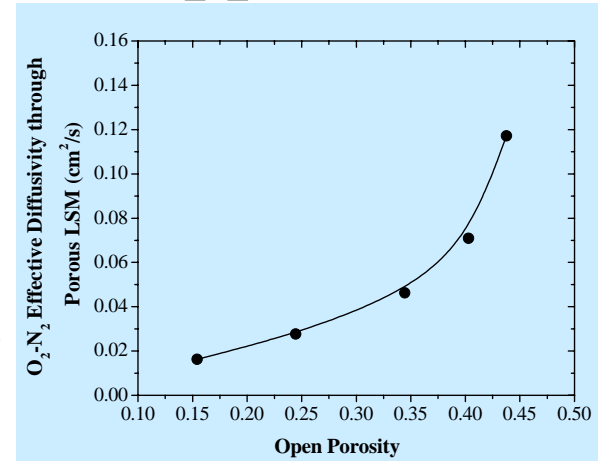
**Higher Polarization at Higher Fuel Utilization**



# Anode Concentration Polarization: Effective Diffusivity vs. Anode Support Porosity



Experimentally  
Measured  $O_2-N_2$   
Effective  
Diffusivity



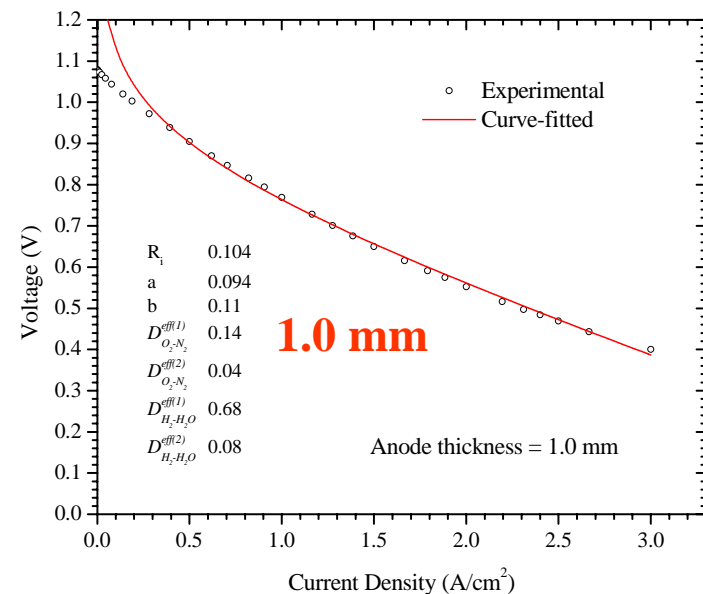
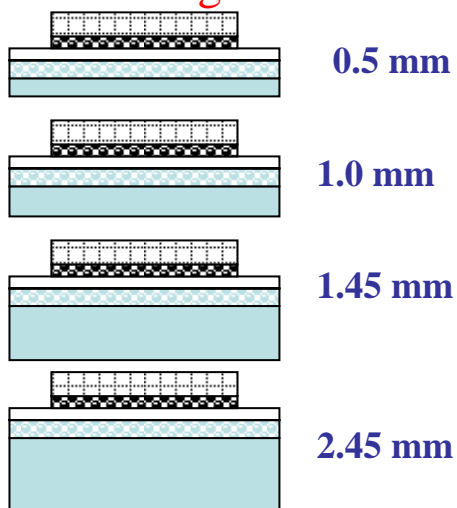
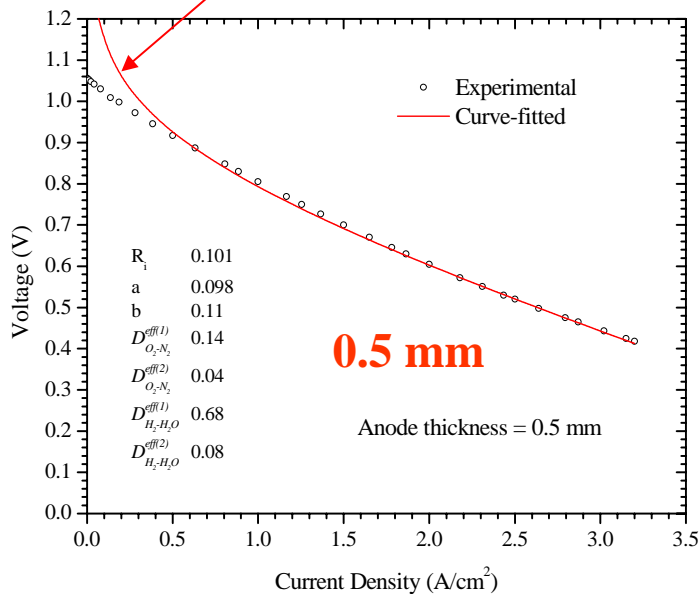
These are  
out-of-cell,  
independent  
measurements

Diffusivities calculated by fitting to experimental data

Anode Support Porosity	$D_{O_2-N_2}^{eff(1)}$ $cm^2/s$	$D_{O_2-N_2}^{eff(2)}$ $cm^2/s$	$D_{H_2-H_2O}^{eff(1)}$ $cm^2/s$	$D_{H_2-H_2O}^{eff(2)}$ $cm^2/s$	Conc. Pola. At 1 A/cm <sup>2</sup> (1 mm)
32%	0.14	0.04	0.22	0.085	125 mV
48%	0.14	0.04	0.68	0.08	75 mV
57%	0.14	0.04	0.75	0.08	72 mV
76%	0.14	0.04	0.82	0.08	70 mV

# Curve Fitting: Anode Support Thickness Varied

Deviation due to the assumption of Tafel equation over the whole range

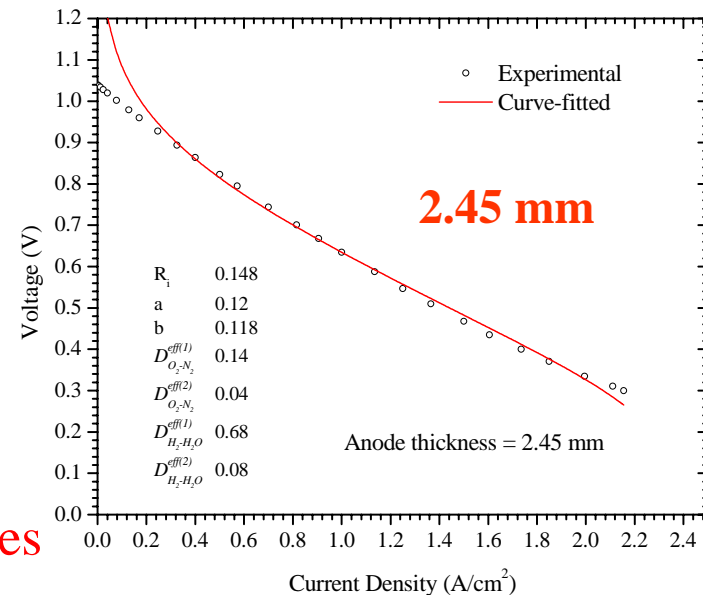
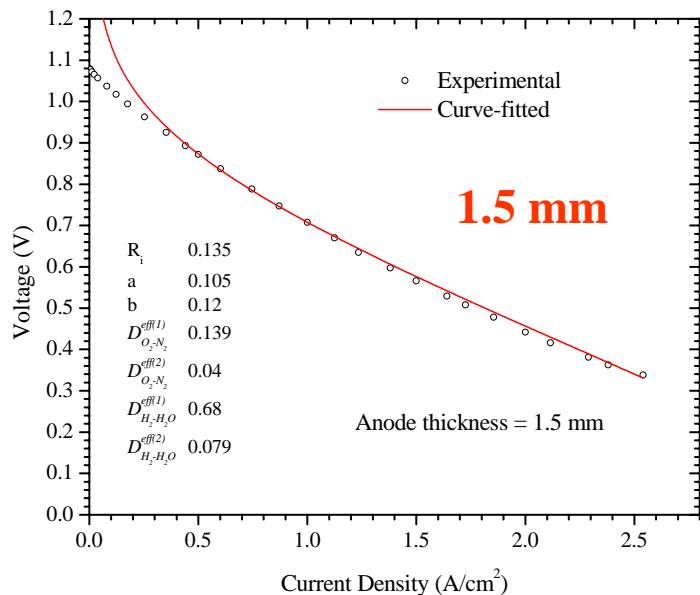


$$D_{H_2-H_2O}^{eff(1)} = 0.68 \text{ cm}^2/\text{s}$$

$$D_{H_2-H_2O}^{eff(2)} = 0.08 \text{ cm}^2/\text{s}$$

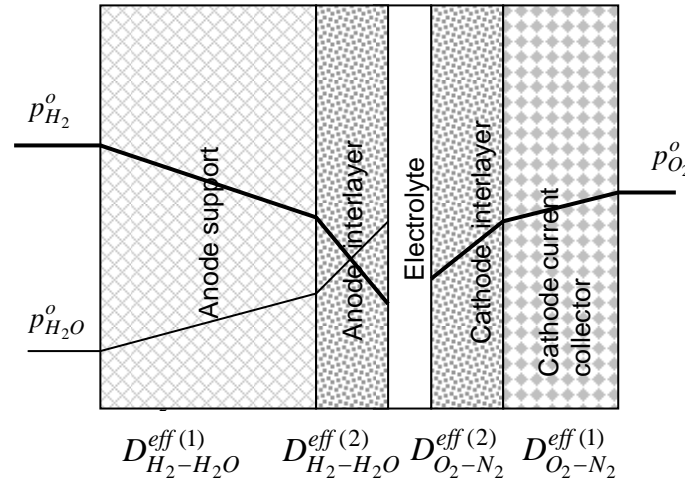
$$D_{O_2-N_2}^{eff(1)} = 0.14 \text{ cm}^2/\text{s}$$

$$D_{O_2-N_2}^{eff(2)} = 0.04 \text{ cm}^2/\text{s}$$



All data could be fitted with above effective diffusivities

# Effective Diffusivities from Fitting to Experimental Cell Data: Anode Thickness Varied (Porosity ~48%)



Anode Support Thickness	$D_{O_2-N_2}^{eff(1)}$ cm <sup>2</sup> /s	$D_{O_2-N_2}^{eff(2)}$ cm <sup>2</sup> /s	$D_{H_2-H_2O}^{eff(1)}$ cm <sup>2</sup> /s	$D_{H_2-H_2O}^{eff(2)}$ cm <sup>2</sup> /s	Conc. Pola. At 1 A/cm <sup>2</sup>
0.5 mm	0.14	0.04	0.68	0.08	55 mV
1.0 mm	0.14	0.04	0.68	0.08	75 mV
1.5 mm	0.14	0.04	0.68	0.08	90 mV
2.45 mm	0.14	0.04	0.68	0.08	115 mV

# Anode Support Thickness Varied: Conclusions

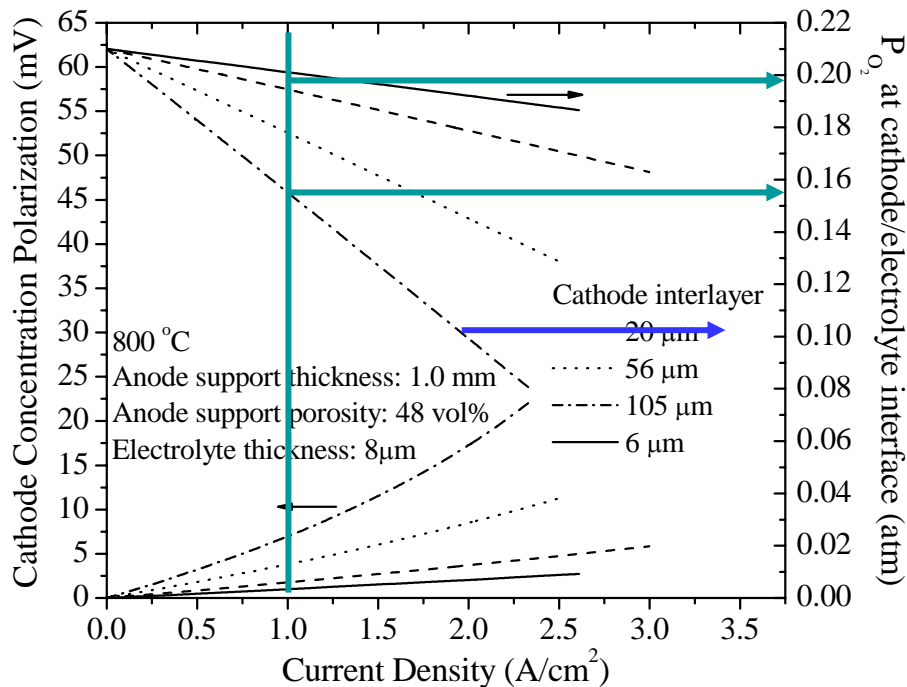
- 1) The thicker the anode support, the lower the performance.
- 2) All of the voltage vs. current density plots could be fitted to one set of effective diffusivities.
- 3) The main contribution is from anode concentration polarization – but not entirely.
- 4) Other contributions from: (a) Ohmic (b) Activation polarization.

The thicker the anode support, the lower the interface hydrogen pressure at a given current density, the poorer the electrocatalysis.

Anode Support Thickness	Ohmic ( $\Omega\text{cm}^2$ )	Tafel Parameter 'a'	Tafel Parameter 'b'	Exchange Current Density ( $\text{mA}/\text{cm}^2$ )
0.5 mm	0.101	0.098	0.11	~410
1.0 mm	0.104	0.094	0.11	~425
1.5 mm	0.135	0.105	0.12	~417
2.45 mm	0.148	0.12	0.118	~ <b>362</b>

The above for low fuel utilization. At higher fuel utilization, both concentration and activation polarization are higher.

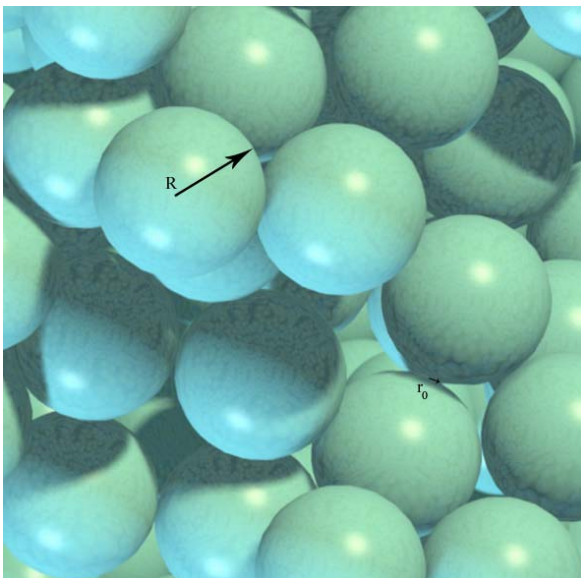
# Cathode Concentration Polarization: Effect of Cathode Interlayer Thickness



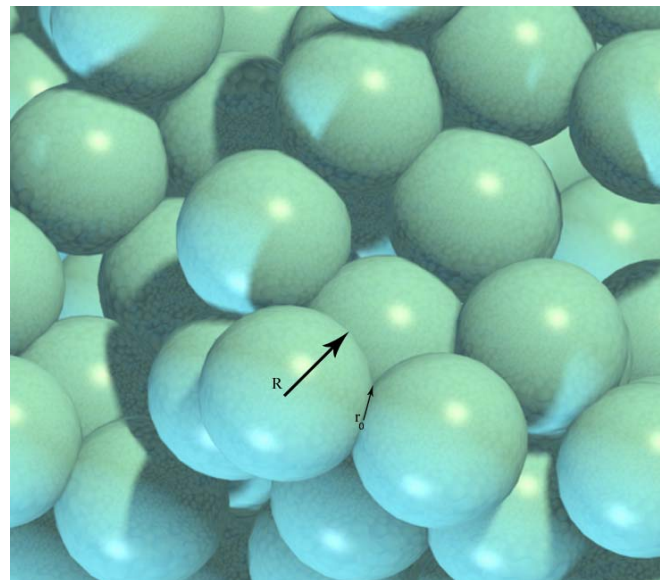
**At high cathode interlayer thicknesses and/or high current densities, oxygen partial pressure at the cathode/electrolyte interface can be quite low -Implications concerning cathodic activation polarization**

**Estimated maximum cathode concentration polarization at 1 A/cm² is <10 mV**

# Transport Properties of Porous Bodies: Implications Concerning Electrode Activation Polarization

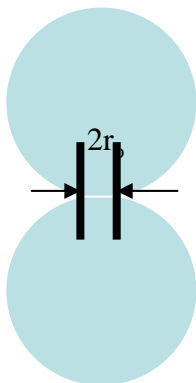


Narrow Necks



Wide Necks

## Morphology



Relative Neck Size

$$\alpha = r_o / R$$

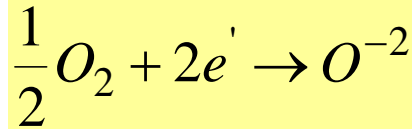


**Low Conductivity**  
**High Resistivity**

**High Conductivity**  
**Low Resistivity**

# A Composite Cathode: Electrode Morphology

Cathodic Reaction

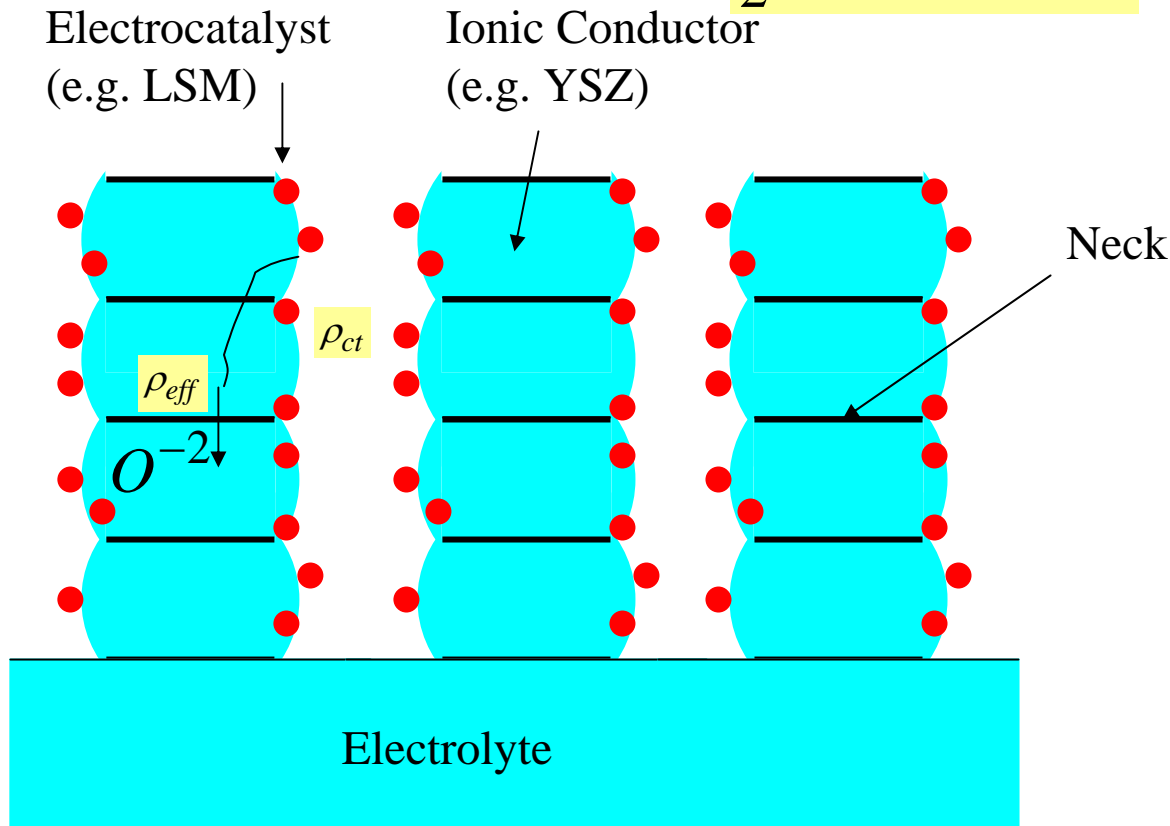


Effective Activation  
Polarization Resistance of  
Composite Electrodes

$$R_p \approx \sqrt{\frac{\rho_{eff} \rho_{ct} d}{(1 - V_v) \ell_{TPB}}}$$

$\rho_{eff}$  Effective Resistivity

$\rho_{ct}$  Charge Transfer Resistivity



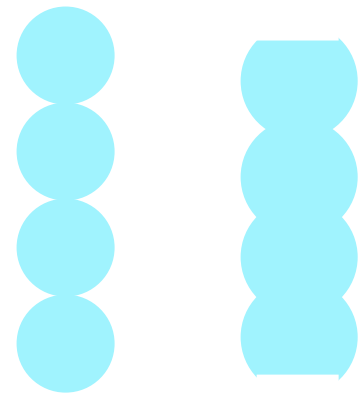
LSM phase is contiguous –

appears noncontiguous on a two-dimensional cut

The same effect of morphology in the anode.

The same effect of morphology in

Single phase MIEC cathodes (LSC, LSF, LSCF)



Narrow Necks High  $\rho_{eff}$

Wide Necks Low  $\rho_{eff}$

# Effective Resistivity of Porous Bodies: No Space Charge Effect Included

$$\rho_{eff} \approx \frac{\rho_g}{2\sqrt{1-\alpha^2}} \ln \left\{ \frac{1+\sqrt{1-\alpha^2}}{1-\sqrt{1-\alpha^2}} \right\} + \frac{\rho_{gb}\delta_{gb}}{2R\alpha^2\sqrt{1-\alpha^2}}$$

$\rho_g$  = Grain Resistivity

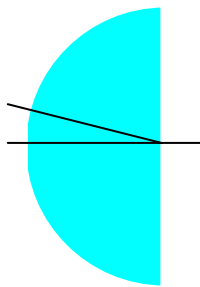
$\rho_{gb}$  = Grain Boundary Resistivity

$\delta_{gb}$  = Grain Boundary Thickness

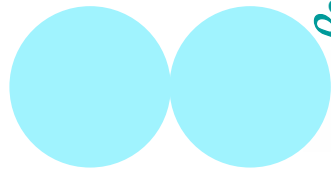
$\alpha$  = Neck radius/Particle radius

Note that as  $\alpha \rightarrow 0$ , both terms become singular

$$\rho_{eff} \approx \rho_g \ln \left\{ \frac{2}{\alpha} \right\} + \frac{\rho_{gb}\delta_{gb}}{2R\alpha^2}$$

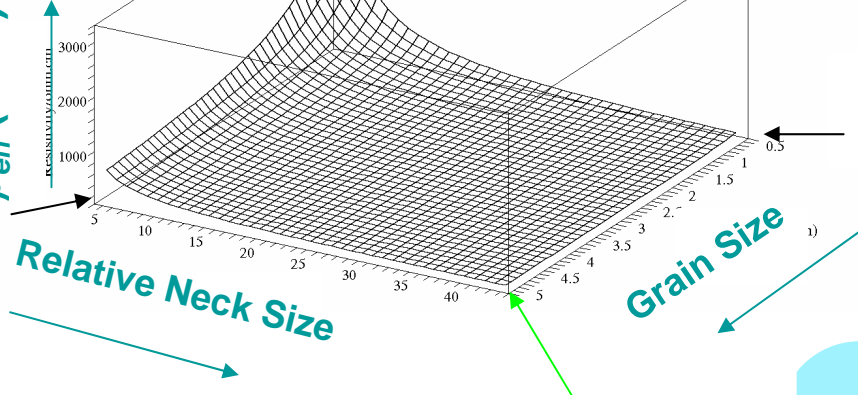


Angle

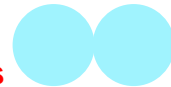


$\rho_{eff} (\Omega cm)$

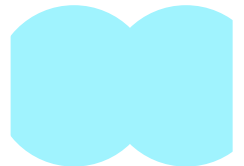
Relative Neck Size



Small Grains  
Narrow Necks



Large Grains  
Wide Necks

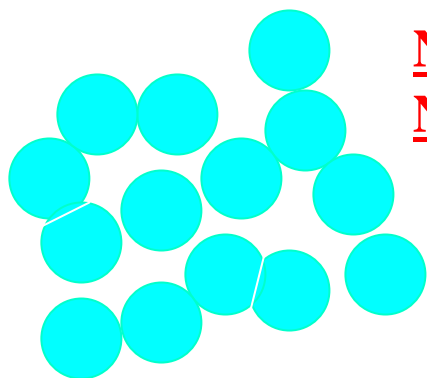


**Implications: Narrow neck size has a profoundly adverse effect on conduction – and on electrocatalytic activity of porous electrodes.**



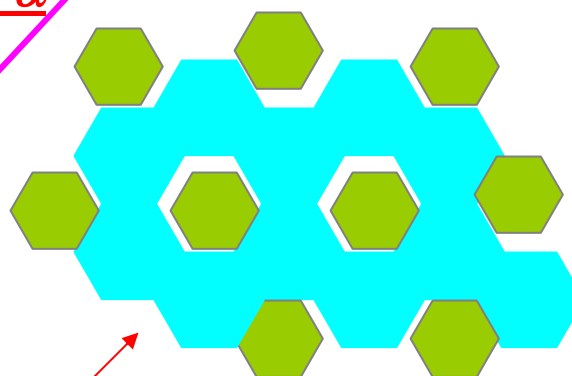
# Fabrication of Porous $\text{Sm}_2\text{O}_3$ -doped $\text{CeO}_2$ (SDC) or $\text{Sc}_2\text{O}_3$ -doped $\text{CeO}_2$ (ScDC): Fabrication of Electrode Structures with Wide Necks

Conventional



Narrow  
Necks; small  $\alpha$

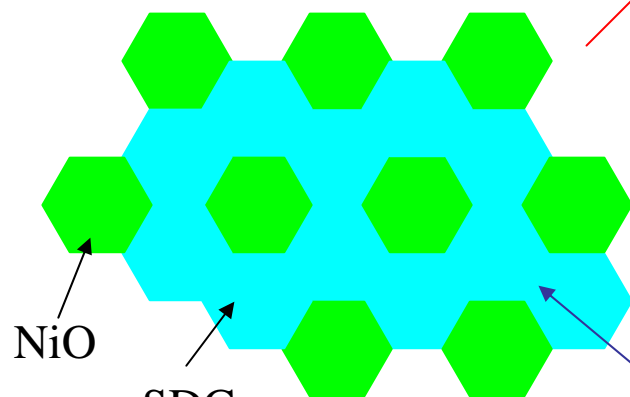
SDC + Ni



Reduction  
of NiO to Ni

Leaching of Ni

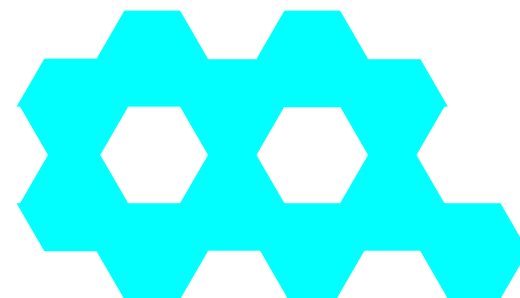
SDC + NiO



Wide necks

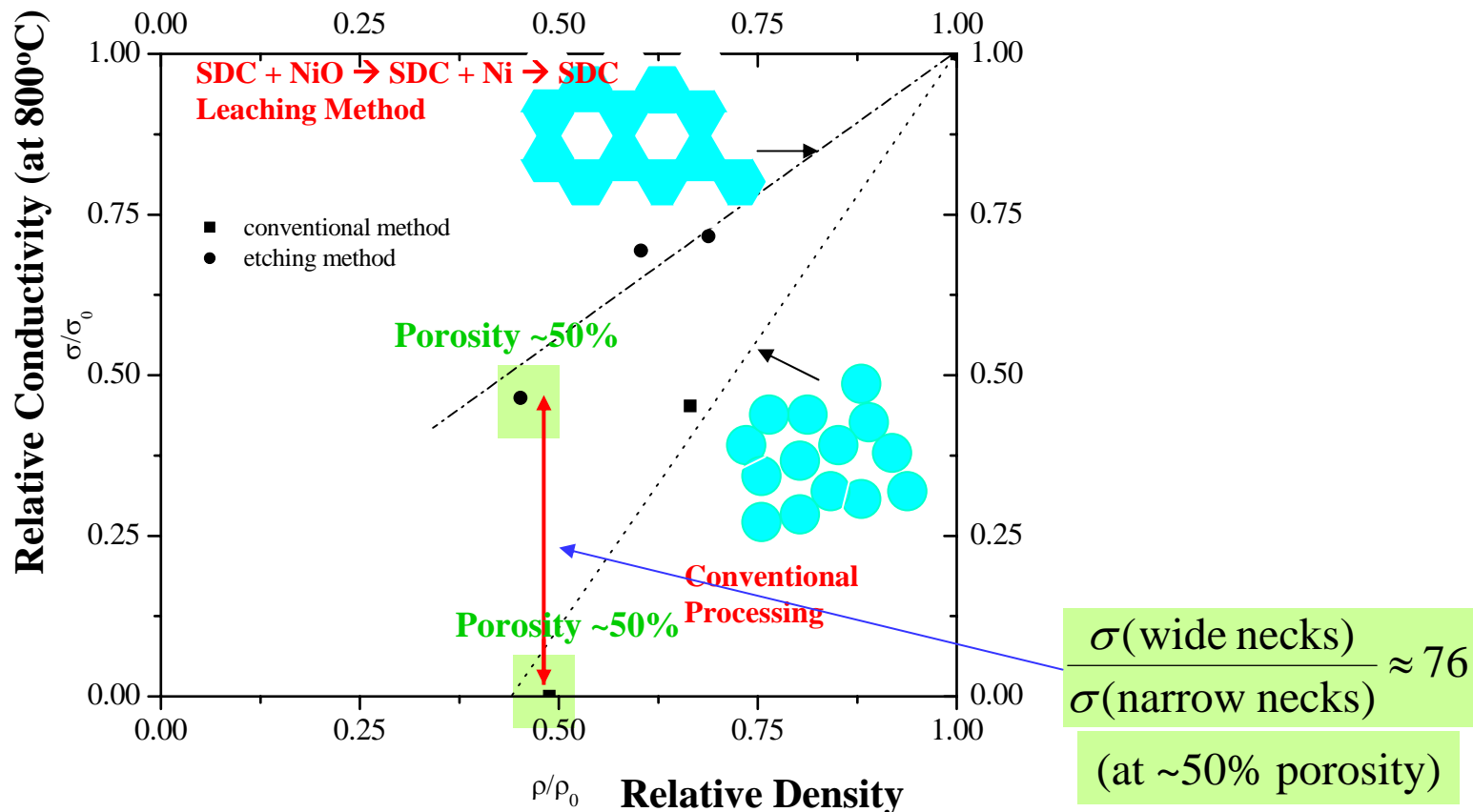
Wide necks;  
large  $\alpha$

Porous SDC

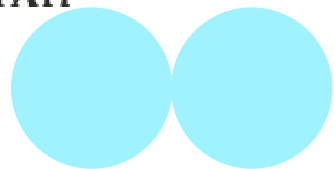


# Conductivity of Porous Bodies:

## Effect of Neck Radius: Experimental Results

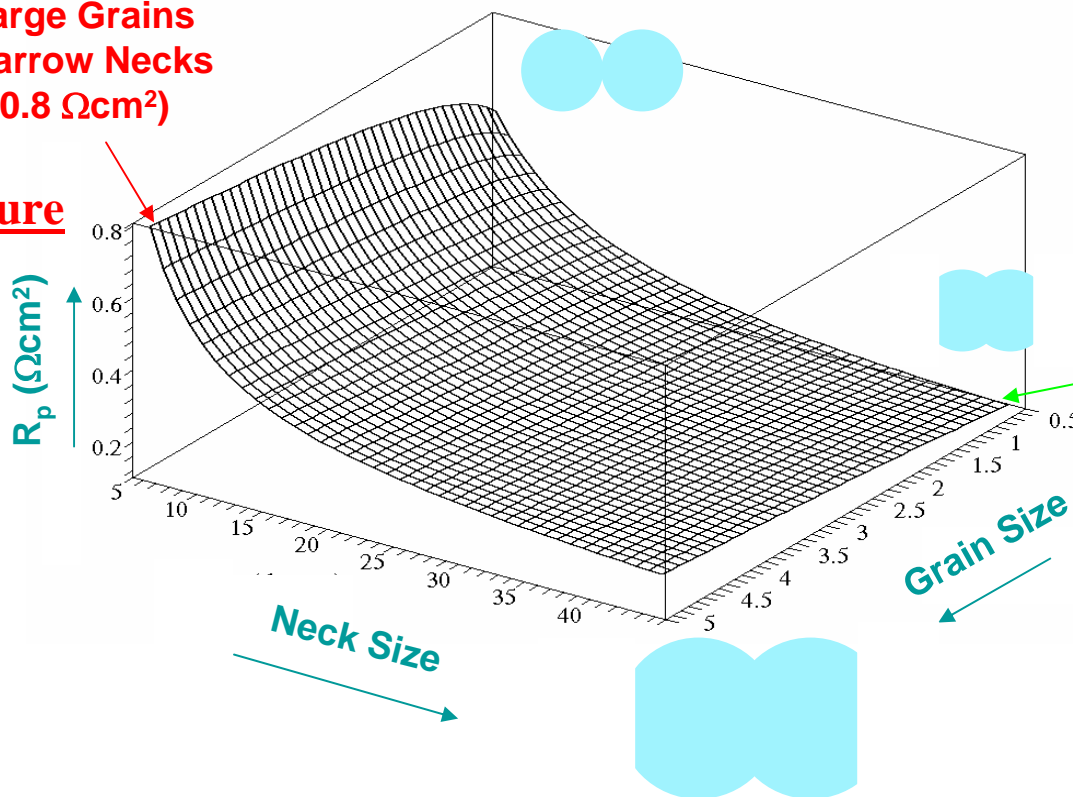


# Calculated Activation Polarization Resistance



Large Grains  
Narrow Necks  
(~0.8  $\Omega\text{cm}^2$ )

Undesired  
Microstructure



$$R_p \approx \sqrt{\frac{\rho_{eff} d \rho_{ct}}{(1 - V_v) \ell_{TPB}}}$$

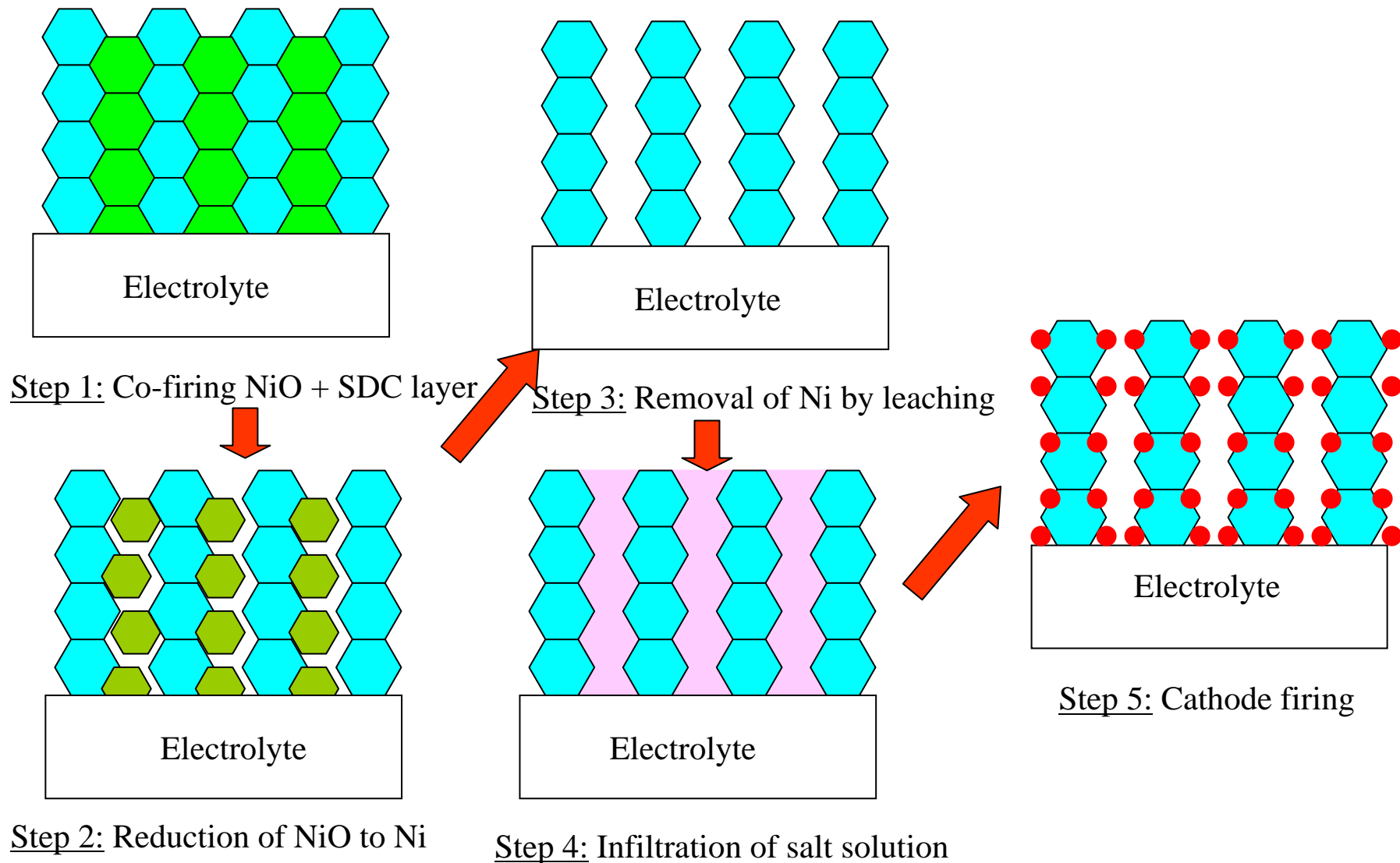
Small Grains  
Wide Necks  
(~0.1  $\Omega\text{cm}^2$ )

Preferred  
Microstructure

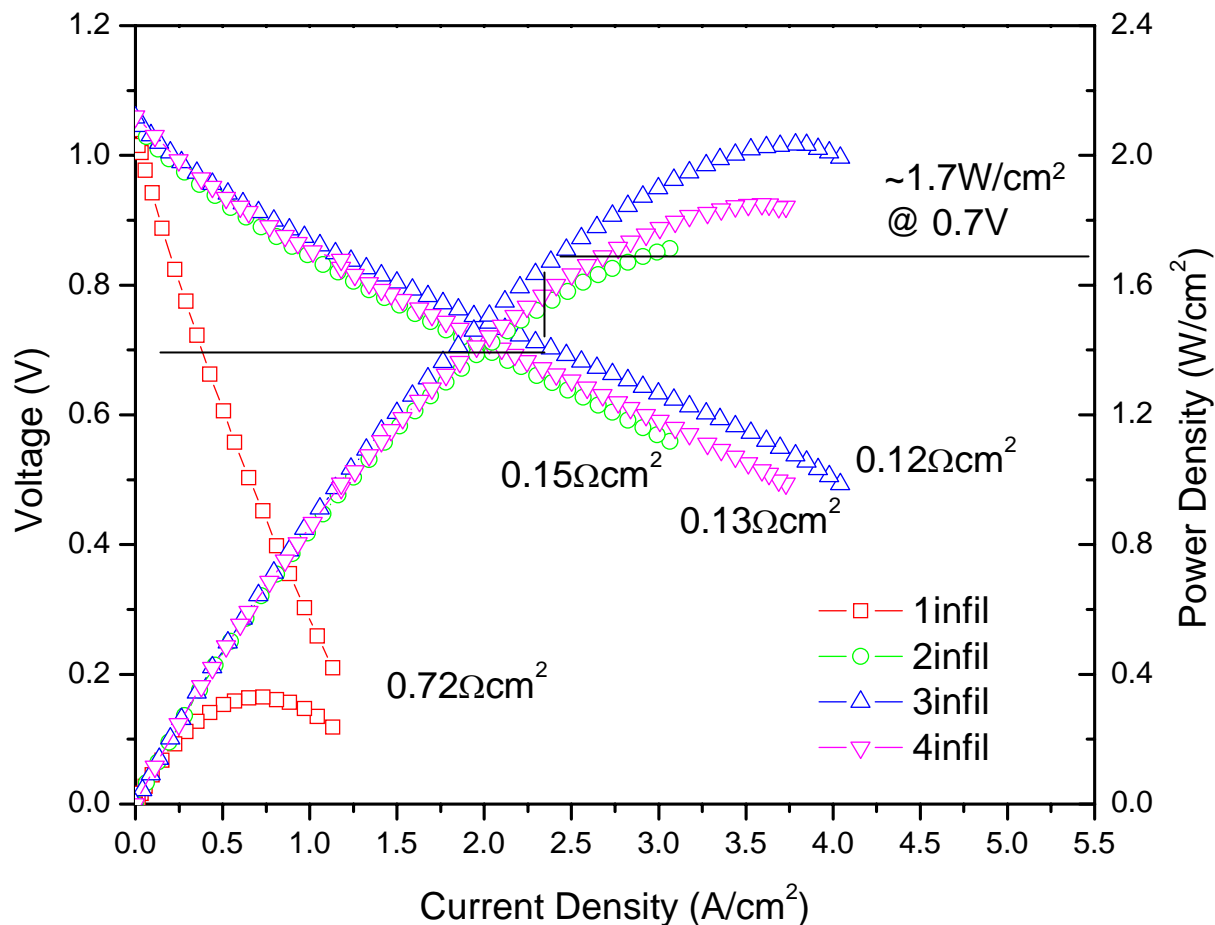
Conclusion: Electrode particles should be fine with wide inter-particle necks.

# Cathodes with Wide Inter-particle Necks

## Cathode Preparation by Reduction and Infiltration



# Some Results on Cells with LSC + YSZ Cathodes Made by Infiltration



H<sub>2</sub>-Air, 800°C, low fuel utilization: 2 cm<sup>2</sup> active area

Rest of the Parameters Standard (not necessarily optimized)

Anode Thickness ~1 mm

# Chemical Effects in Activation Polarization

## Composite (Electrocatalyst, e.g. LSM + Ionic Conductor, e.g. YSZ) Cathodes

- Type of Electrocatalyst (material, composition).
- Electrolyte (e.g. YSZ, Ceria).
- Effect of atmosphere (e.g. oxygen partial pressure).
- Temperature

$$R_p \approx \sqrt{\frac{\rho_{eff} d \rho_{ct}}{(1 - V_v) \ell_{TPB}}}$$

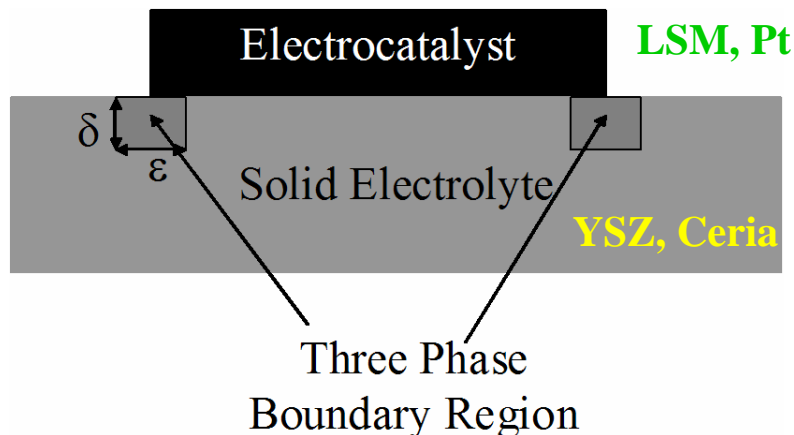
$\ell_{TPB}$  Three Phase Boundary Length (cm<sup>-1</sup>)  
Charge Transfer Resistance

$$R_{ct} = \frac{\rho'_{ct} \delta}{\varepsilon \ell_{TPB}} = \frac{\rho_{ct}}{\ell_{TPB}}$$

Charge Transfer Resistivity

$$\rho_{ct} = \frac{\rho'_{ct} \delta}{\varepsilon}$$

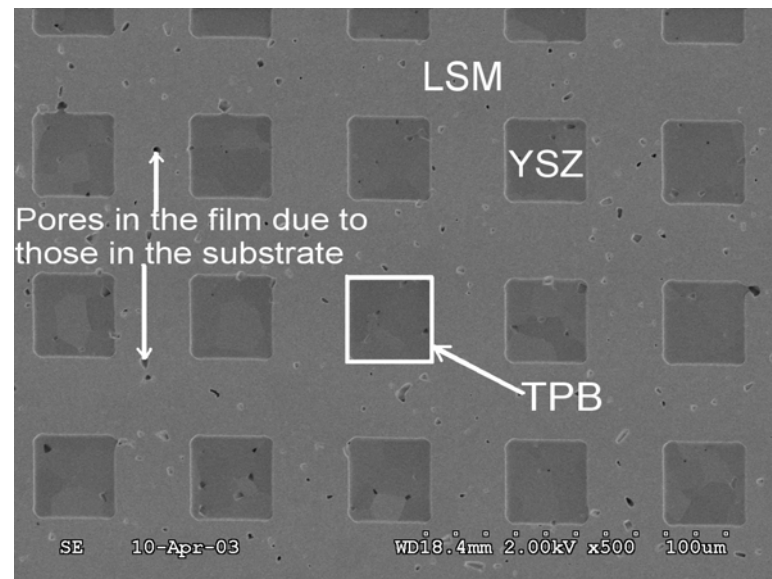
$\rho_{ct}$  Depends on  
1) Materials  
2) Atmosphere  
3) Temperature



# Patterned Electrodes for the Measurement of Charge Transfer Resistivity

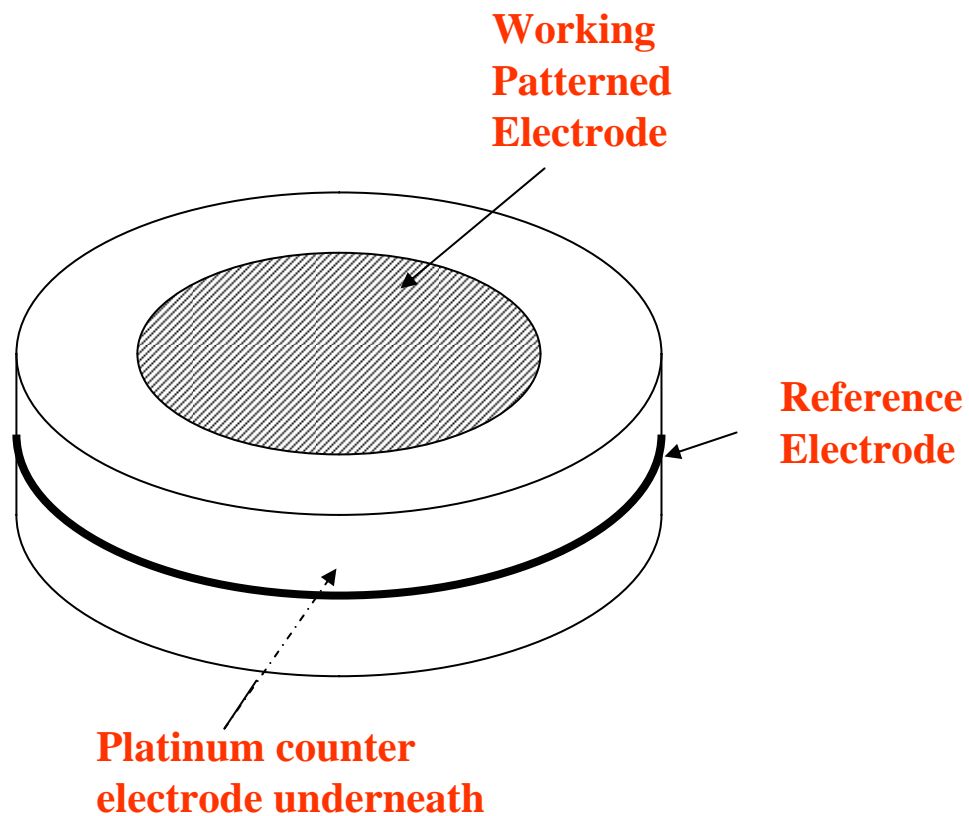
$$\rho_{ct}$$

- Use of photomicro lithography for the deposition of patterned electrodes of known TPB length.
- Patterned electrodes for the measurement of charge transfer resistivity of LSM and Pt on YSZ.
- Effect of oxygen partial pressure.
- Effect of temperature.



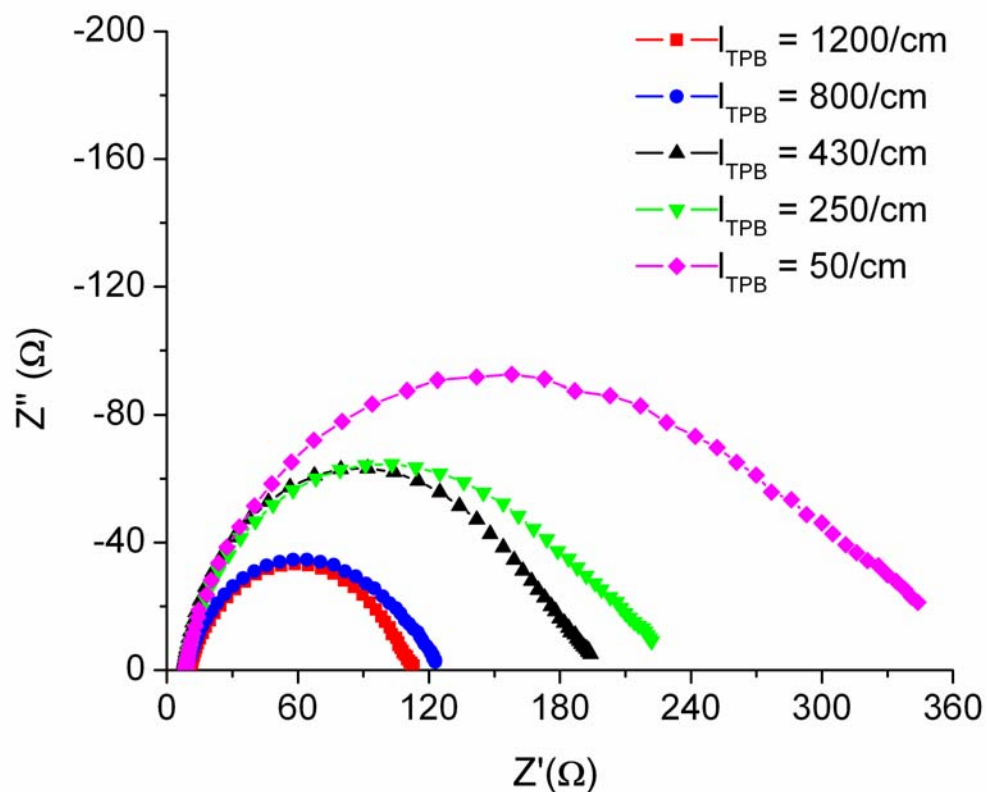
- 1) Deposit patterned electrodes on an electrolyte disc.
- 2) Heat to the desired temperature.
- 3) Expose to the desired oxygen partial pressure.
- 4) Measure impedance spectra under zero bias.

# Testing Geometry

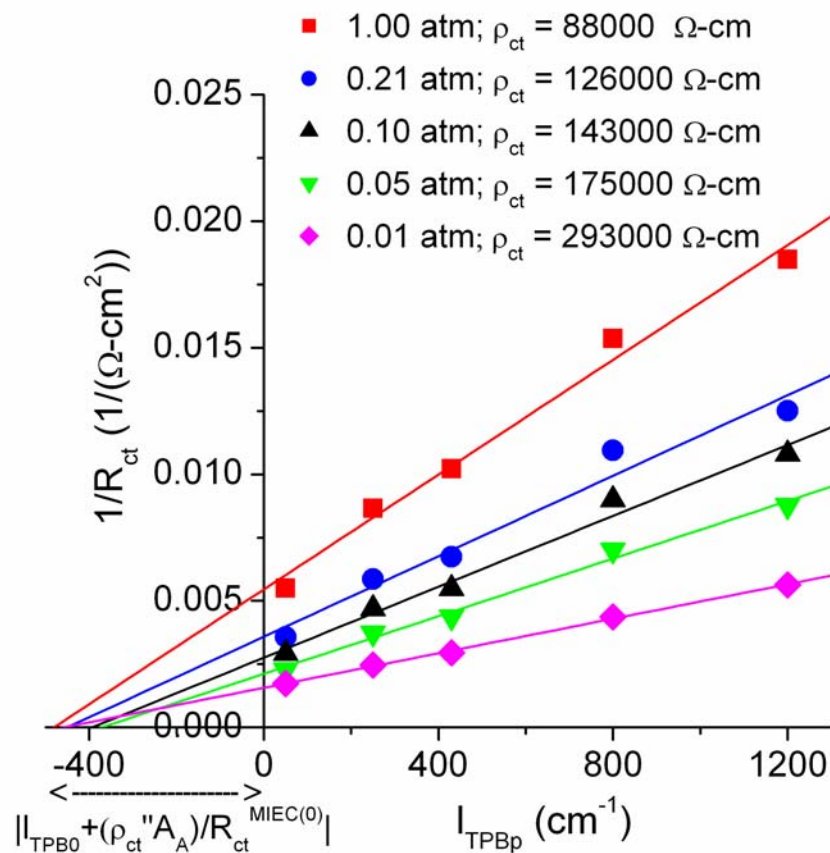




# Impedance Spectra at 800°C in Air for LSM/YSZ for Several TPB Length

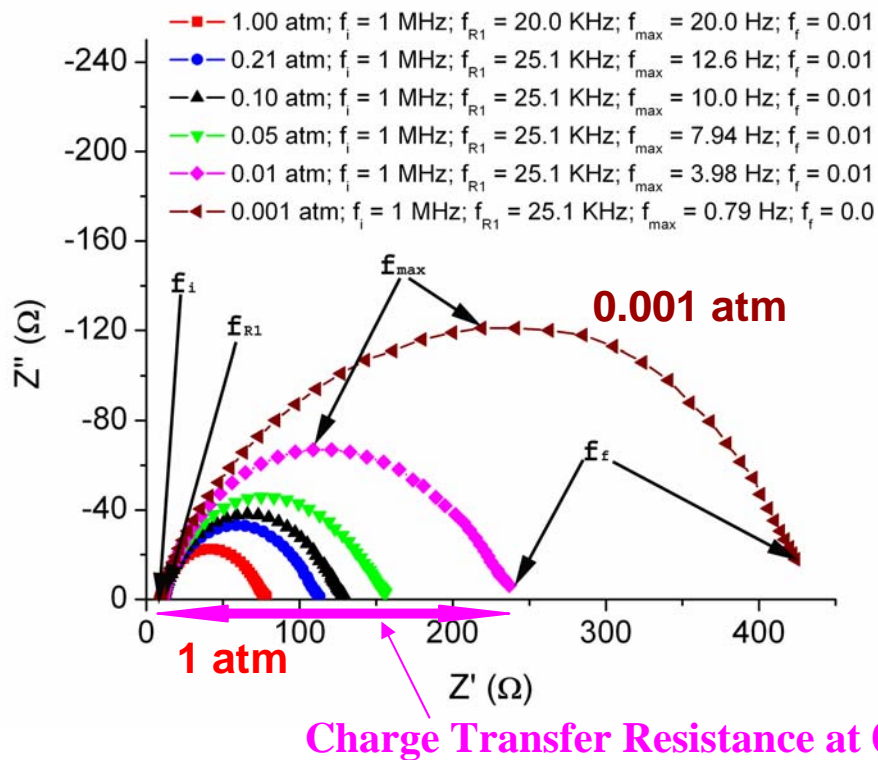


# $1/R_{ct}$ vs. $l_{TPB}$

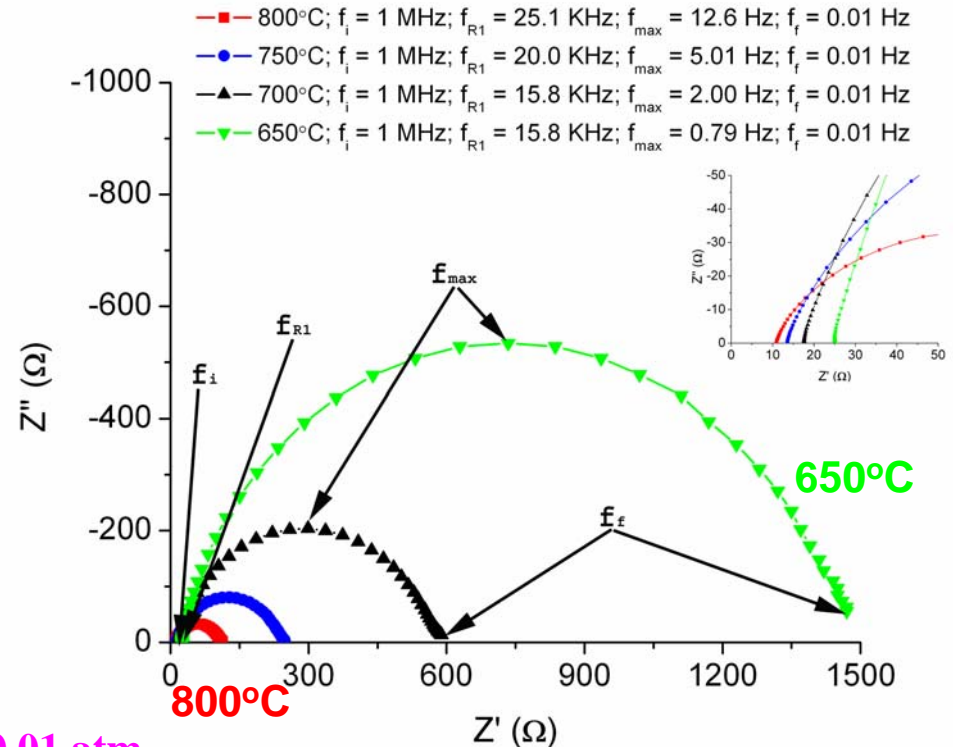


**$1/R_{ct}$  vs.  $l_{TPB}$  is linear; thus, most of the charge transfer occurs at TPB.  
Nonzero intercept mainly due to unintended TPB due to pores in the film.**

# Effect of Oxygen Partial Pressure and Temperature on the Polarization Resistance of LSM on YSZ



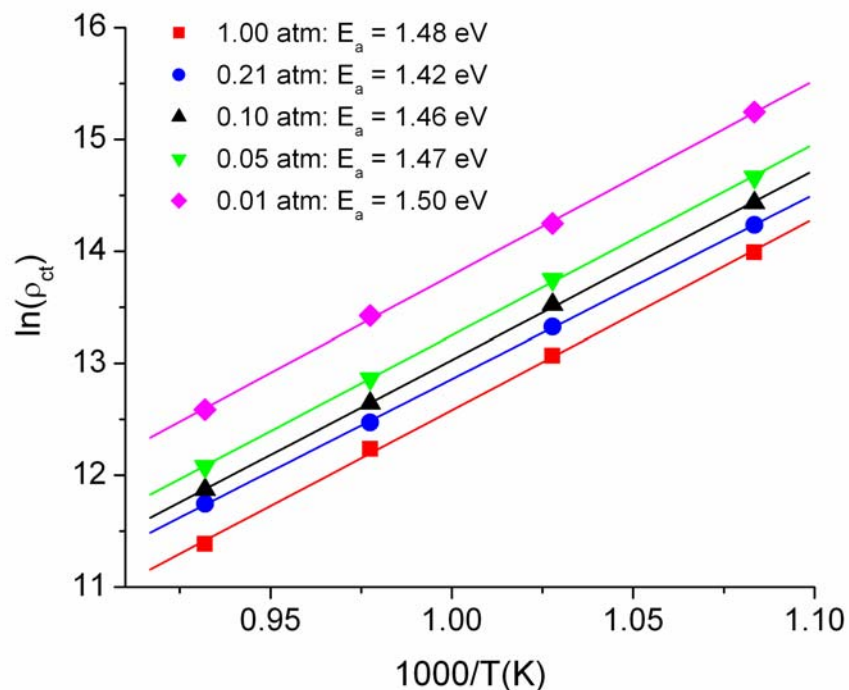
The higher the oxygen partial pressure, the lower the polarization resistance



The higher the temperature, the lower the polarization resistance

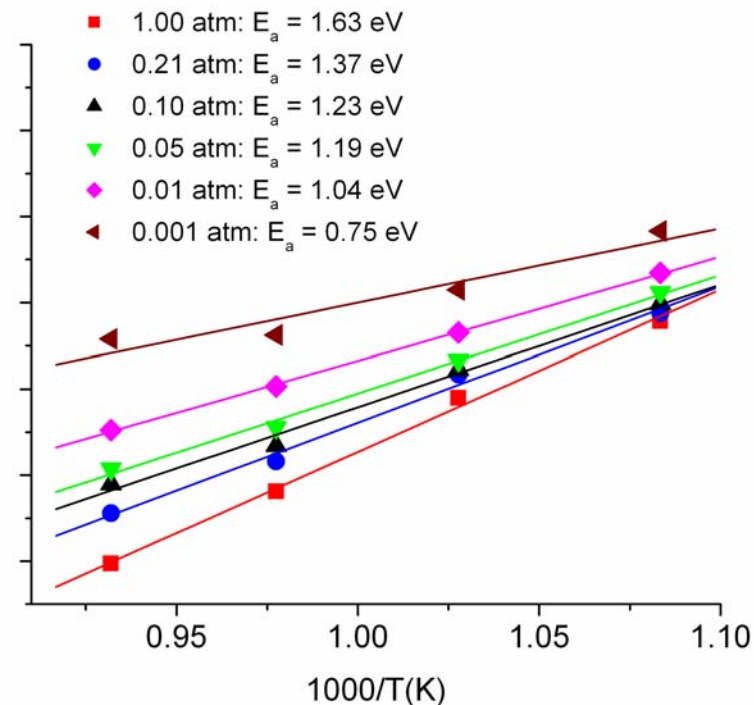
# Arrhenius Plots of $\rho_{ct}$ for LSM/YSZ and Pt/YSZ at Various $pO_2$

## LSM/YSZ



Activation Energy independent of  $pO_2$ : Weak adsorption

## Pt/YSZ



Activation Energy decreases with decreasing  $pO_2$ : Stronger adsorption

# Charge Transfer Resistivity, $\rho_{ct}$ , of LSM and Pt on YSZ as a Function of $pO_2$ and Temperature

LSM/YSZ

$$\frac{\rho_{ct}(\text{LSM/YSZ})}{\rho_{ct}(\text{Pt/YSZ})} \approx 24$$

At 800°C

$$\frac{\rho_{ct}(\text{LSM/YSZ})}{\rho_{ct}(\text{Pt/YSZ})} \approx 29$$

At 650°C

Temp $pO_2$	1 atm	0.21 atm	0.1 atm	0.05 atm	0.01 atm
800°C	88000	126000	143000	176000	293000
750°C	206000	261000	310000	386000	676000
700°C	474000	613000	746000	935000	1540000
650°C	1190000	1520000	1850000	2330000	4170000

## Conclusion:

1) Pt is 25 to 30 times better than LSM

2) Strong  $pO_2$  dependence for both

3) Strong temperature dependence for both

## Pt/YSZ

Temp $pO_2$	1 atm	0.21 atm	0.1 atm	0.05 atm	0.01 atm	0.001 atm
800°C	2900	5200	7300	8700	13700	39200
750°C	6700	9500	11400	14100	22700	41100
700°C	19900	26100	27600	30600	42400	69400
650°C	48200	52900	59000	67300	84400	137500

# Calculation of The Polarization Resistance of LSM/YSZ Composite Cathodes in air at 800°C

$$R_p \approx \sqrt{\frac{\rho_{eff} d \rho_{ct}}{(1 - V_v) \ell_{TPB}}}$$

$$R_p \approx \sqrt{\frac{\rho_{eff} d R_{ct}}{(1 - V_v)}}$$

where

$$R_{ct} = \frac{\rho_{ct}}{\ell_{TPB}}$$

Effective Exchange Current Density

$$i_o = \frac{RT}{4FR_p}$$

$$d \sim 1 \mu\text{m}$$

$$V_v \sim 0.25$$

$$\ell_{TPB} \sim 10,000 \text{ cm}^{-1}$$

$$\rho_{eff} \sim 30 \Omega\text{cm}$$

$$\rho_{ct} \sim 126,000 \Omega\text{cm}$$

$$R_{ct} \sim 12.6 \Omega\text{cm}^2$$



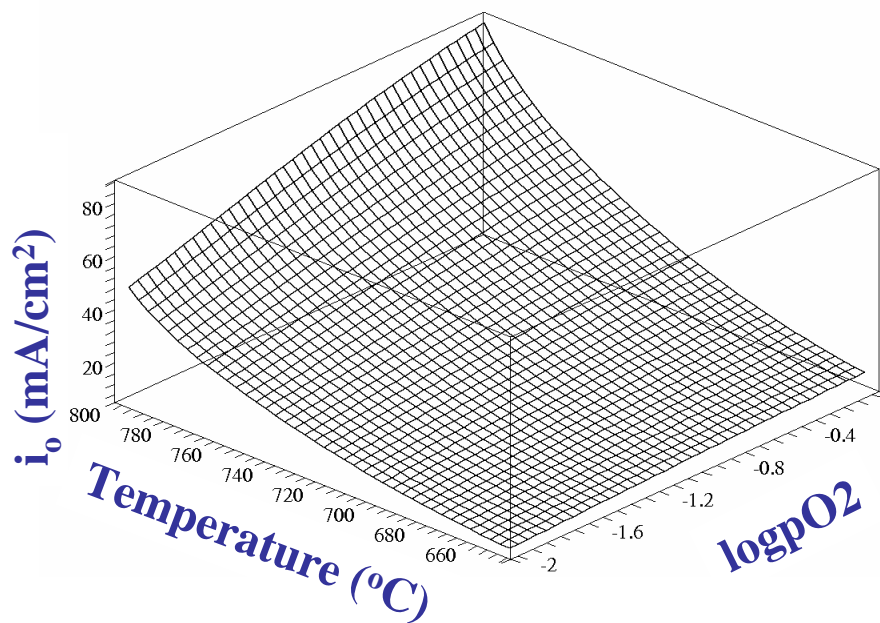
A decrease by a factor of 40

$$R_p \sim 0.224 \Omega\text{cm}^2$$

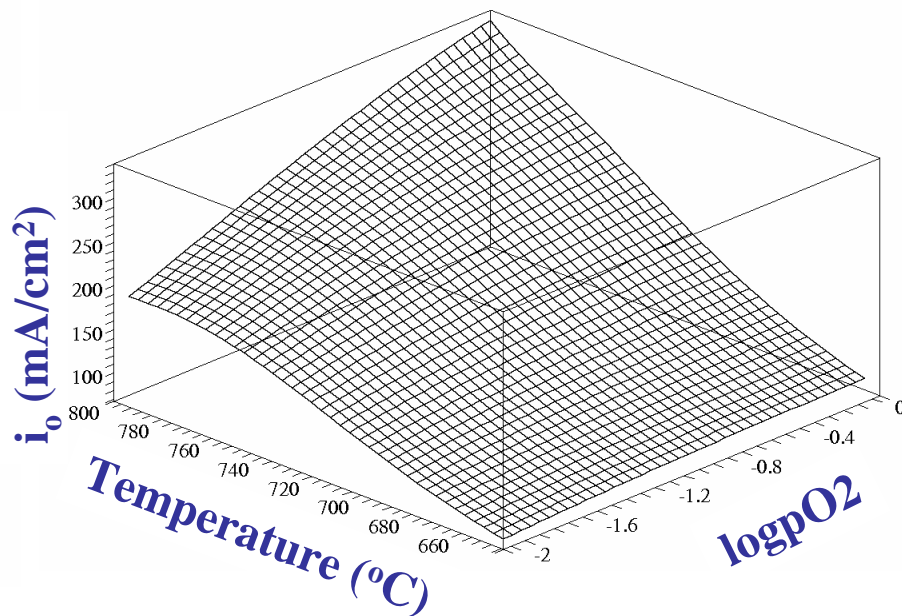
$$i_o \sim 103 \text{ mA/cm}^2$$

# Calculated Effective Exchange Current Densities for LSM/YSZ and Pt/YSZ Composite Cathodes as Function of Temperature and Oxygen Partial Pressure

**LSM/YSZ**



**Pt/YSZ**

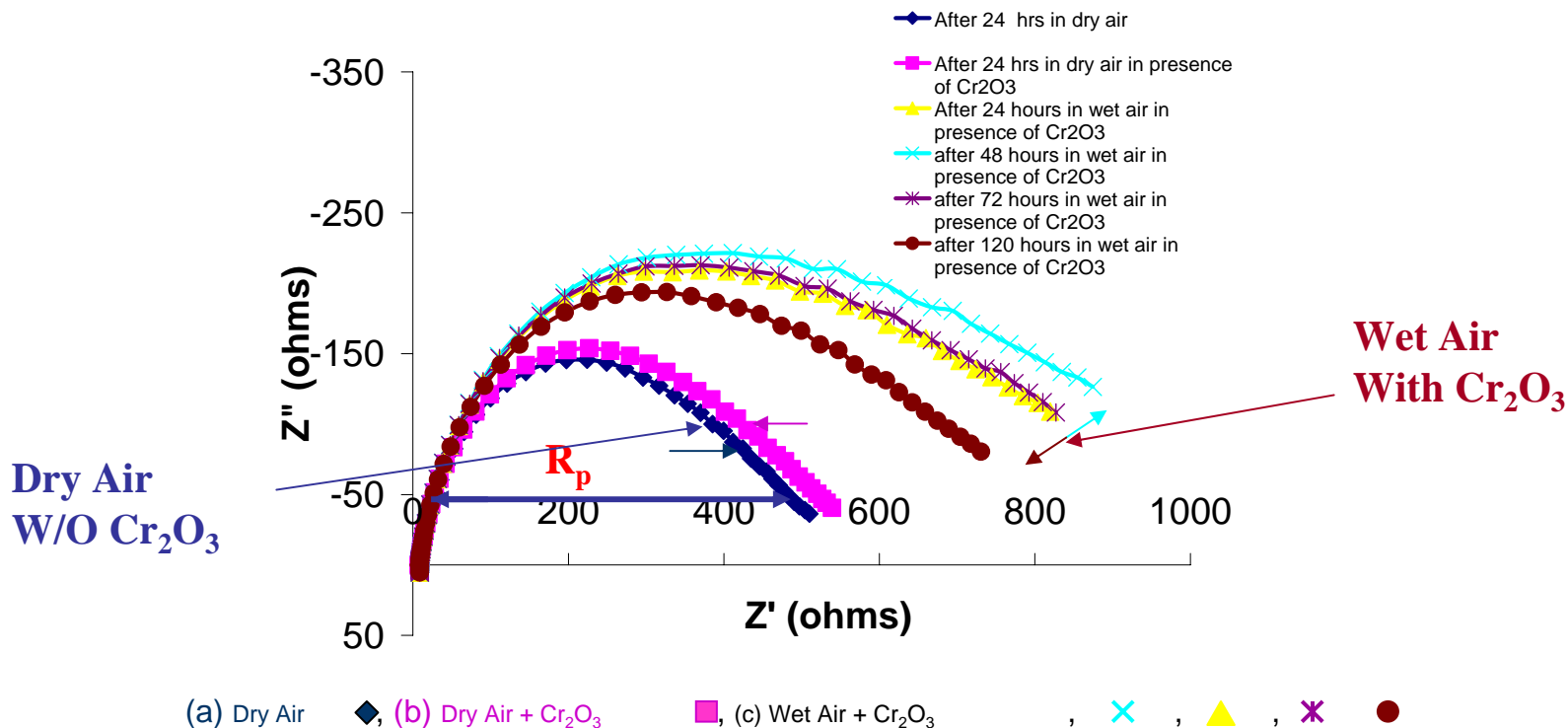


$d = 2$  microns

$V_v = 0.25$

$I_{TPB} = 10,000 \text{ cm}^{-1}$

# Patterned LSM Electrodes for the Investigation of Chromium Poisoning: Preliminary Results



Polarization resistance increased from ~500 Ohms to ~1000 Ohms after exposure to  $\text{Cr}_2\text{O}_3$  in flowing wet air at 800°C for 48 hours.



# Single Phase Mixed Ionic Electronic Conducting (MIEC) Cathodes

- Ionic and electronic transport occurs through a single phase material. LSC, LSF, LSCF, etc.
- General features of the model are similar to those of composite cathodes, although the experimentally measured parameters are different.
- Composite cathodes: Ionic conductivity of the ionic conductor, grain size, charge transfer resistivity, porosity, and three phase boundary length.
- Single phase MIEC cathodes: Oxygen diffusion coefficient, surface exchange coefficient, porosity, and specific pore surface area.

$$R_p \approx \sqrt{\frac{\rho_{eff} d \rho_{ct}}{(1 - V_v) \ell_{TPB}}}$$

Two Phase Composite MIEC Cathode

$$R_{chem} \approx \frac{RT}{2F^2} \sqrt{\frac{\tau}{(1 - V_v) S_v C_o^2 D k_{exc}}}$$

Single Phase MIEC Cathode

# Relevant Chemical Parameters for Single-Phase MIEC Cathodes

Diffusion Coefficient of Oxygen  $D$

and

Surface Exchange Parameter  $k_{exc}$

## Parameters Easily Measured Experimentally

Chemical Diffusion Coefficient of Oxygen  $\tilde{D}$  cm<sup>2</sup>/s  
and

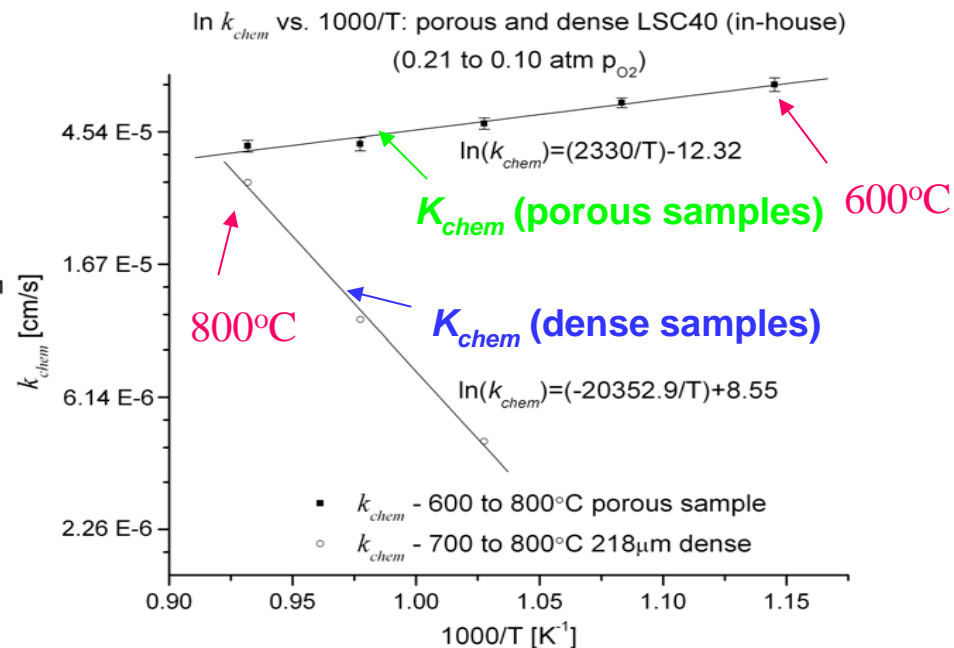
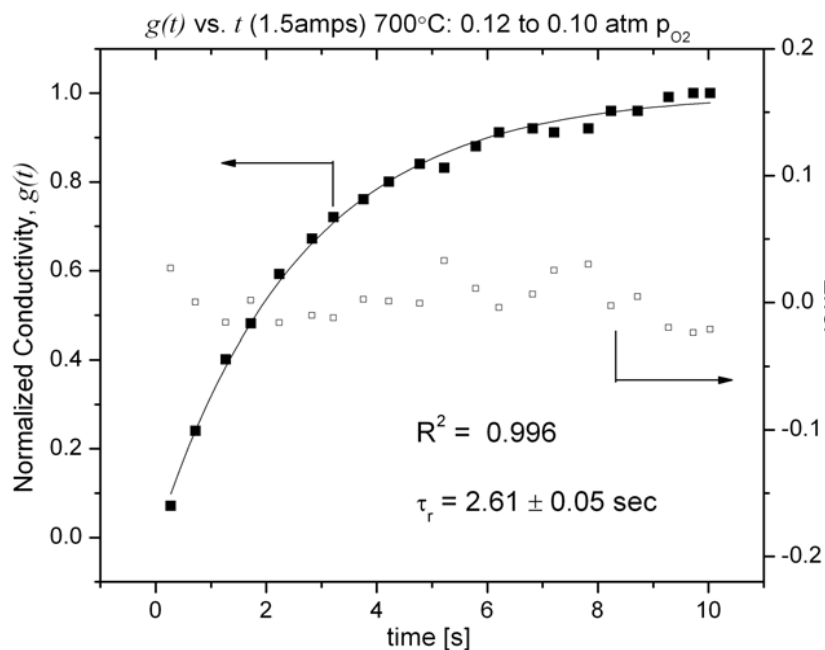
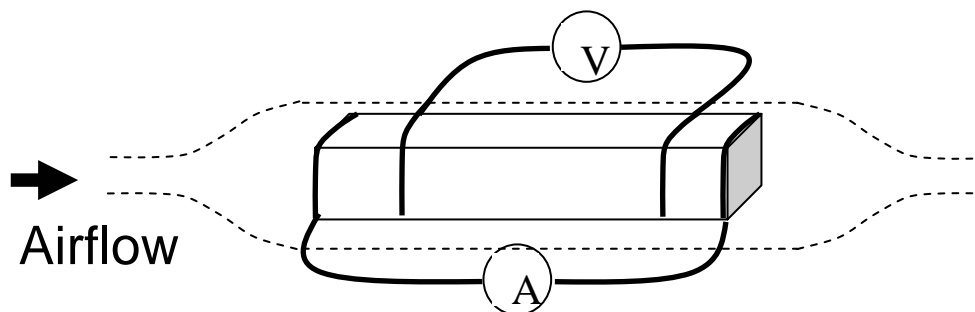
Chemical Surface Exchange Parameter  $k_{chem}$  cm/s

Technique used: Conductivity Relaxation (time response of conductivity change to an abrupt change in oxygen partial pressure)

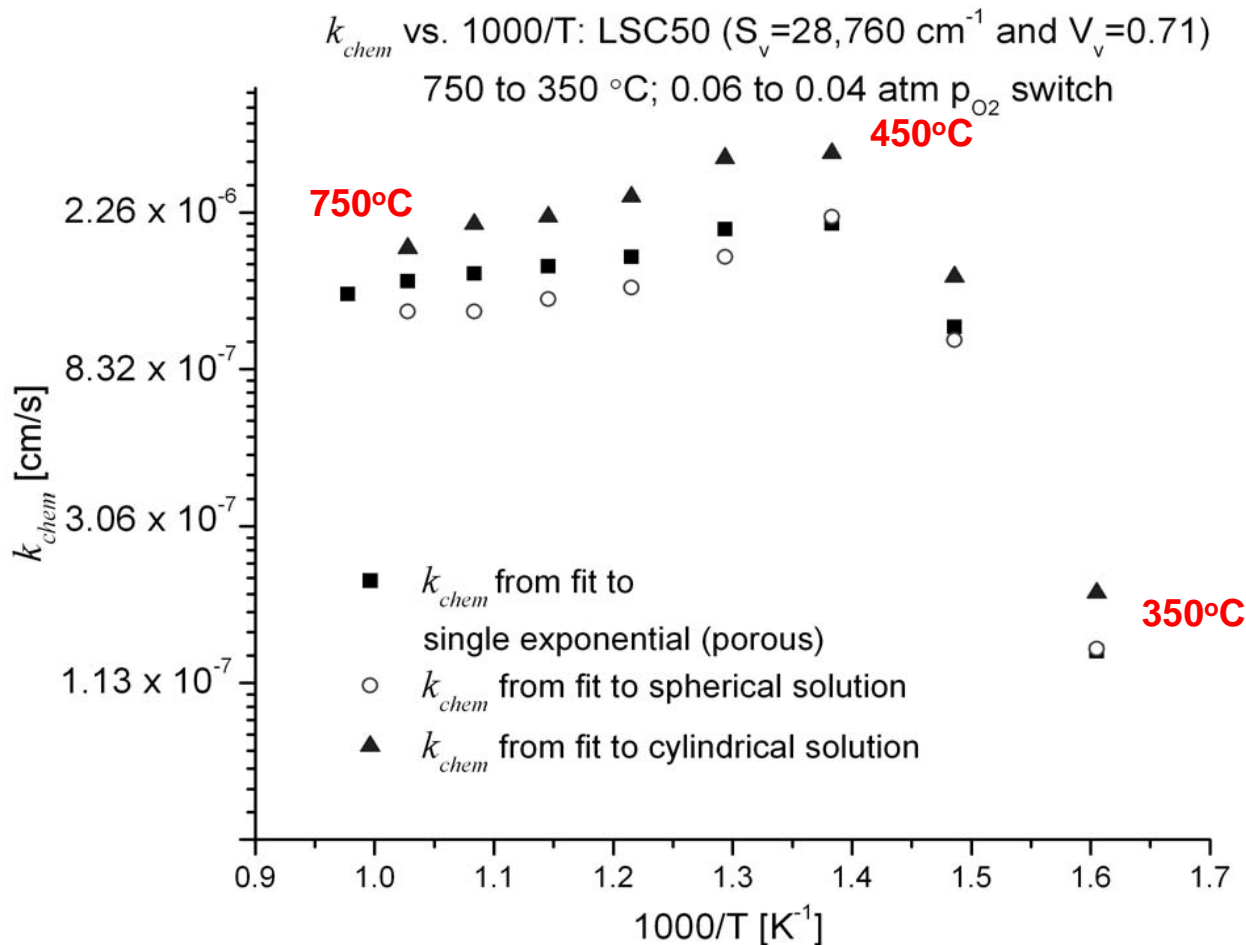
Usual Approach: To use a dense bar-shaped sample.

Our Approach: To use a porous bar-shaped sample.

# Characterization of MIEC Cathodes: Measurement of Surface Exchange Coefficient by Conductivity Relaxation using Porous Bodies



# Measurement of Surface Exchange Coefficient on Porous Bodies: LSC Between 350 and 750°C



Above 450°C,  $k_{chem}$  decreases with increasing temperature.  
Below 450°C,  $k_{chem}$  decreases with decreasing temperature.

Potential implications for SOFC cathodes: Identify materials with high  $k_{chem}$  at lower temperatures.

# Summary: Important Factors for Lowering Electrode Polarization

- Anode Concentration Polarization: High porosity (~50%), low tortuosity, small thickness (~0.4 to ~0.5 mm).
- Cathode Concentration Polarization: High porosity (~50%), low tortuosity, small thickness (~50 to 100 microns).
- Cathode and Anode Activation Polarization - microstructural: Small particle size (nanosize), large neck size.
- Cathode Activation Polarization – chemical: High ionic conductivity, low charge transfer resistivity, large TPB ( $>5,000 \text{ cm}^{-1}$ ), higher oxygen surface coverage at as low an oxygen partial pressure as possible. With MIEC materials: High diffusion coefficient, high surface exchange coefficient.